

Current-induced torques due to compensated antiferromagnets

Paul M. Haney and A.H. MacDonald

Department of Physics, The University of Texas at Austin, Austin, Texas, 78712-0264, U.S.A.

We analyse the influence of current induced torques on the magnetization configuration of a ferromagnet in a circuit containing a compensated antiferromagnet. We argue that these torques are generically non-zero and support this conclusion with a microscopic NEGF calculation for a circuit containing antiferromagnetic NiMn and ferromagnetic Co layers. Because of symmetry dictated differences in the form of the current-induced torque, the phase diagram which expresses the dependence of ferromagnet configuration on current and external magnetic field differs qualitatively from its ferromagnet-only counterpart.

Introduction— Current-induced torques in noncollinear ferromagnetic metal circuits were predicted over 10 years ago [1, 2], and have since been the subject of an extensive and quite successful body of experimental and theoretical research. Almost all studies of current-induced torques consider either their role in ferromagnetic (F) spin valve circuits [3–7] or their influence on magnetic domain wall motion [8–12]. In both cases, the current-induced torques can be understood as following from the transfer of conserved spin angular momentum from current-carrying quasiparticles to the magnetic condensate, hence the term spin-transfer torque. It has recently been predicted that current-induced torques are generically present whenever non-equilibrium quasiparticles interact with non-collinear magnetic order parameters, even [13, 14] in circuits containing only antiferromagnetic (AF) elements. Experiments [15] have established a dependence of unidirectional exchange bias fields on current, providing indirect evidence that current-induced torques are present in AFs. In this Letter we analyse the influence of current-induced torques on a F thin film in a circuit containing a compensated AF. Because of a key difference in symmetry compared to purely F spin-valve circuits, we find that the phase diagram which expresses the dependence of the magnetic configuration of the F on current and external magnetic field differs qualitatively from the familiar F only spin-valve phase diagram [16]. In particular, we find that transport currents can drive the F to a stable steady state with magnetization perpendicular to the AF layer moments. In the following paragraphs we argue on symmetry grounds for the form of the current-induced torque, and explore its robustness by performing a fully microscopic current-induced torque calculation for a circuit containing Co and NiMn layers. We then turn our attention to the construction of the F state phase diagram implied by equations of motion which include the current-induced torque term, and conclude with a discussion of experimental implications.

Current-induced Torques due to Compensated Antiferromagnets— The total current-induced torque acting on a F nanoparticle can always [1] be expressed in terms of the difference between incoming and outgoing spin currents. The presence of a ferromagnet will in general induce a nonzero spin current at the AF-F interface. When spin-polarized electron flux from an AF

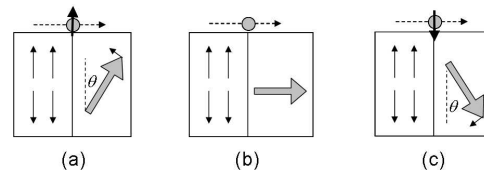


FIG. 1: Current-induced torques due to a compensated antiferromagnet.

with orientation \hat{n}_{AF} enters a F with orientation \hat{n}_F , the spin current entering F will have some component in the \hat{n}_{AF} direction. It follows that, just as in the familiar case where both materials are F, a current-induced torque will act in the plane defined by \hat{n}_{AF} and \hat{n}_F , as illustrated in Fig. (1). (Out of plane torques are also non-zero but tend to be much smaller.) Spin-invariance of the overall circuit implies that the in-plane torque must be an odd function of the angle θ between \hat{n}_F and \hat{n}_{AF} , and that it can therefore be expanded in terms of a sin-only Fourier series, vanishing for both parallel and antiparallel collinear configurations. Most AF materials used in magnetoelectronics are fully compensated, *i.e.* the spin-density sums to zero in every lattice plane perpendicular to the current direction, or at least nearly so. In this case, reversal of the AF moment direction is equivalent to a lateral translation which cannot influence the current-induced torque. It follows that in the compensated AF case the torque is invariant under $\theta \rightarrow \theta + \pi$, restricting its Fourier expansion to terms proportional to $\sin(2n\theta)$. The torque therefore vanishes when \hat{n}_F is perpendicular to \hat{n}_{AF} , and undergoes a sign change for $\theta \rightarrow \pi - \theta$, as illustrated in Fig. (1). The property that the torque acting on a F due to a compensated AF vanishes not only for collinear but also for perpendicular orientations is primarily responsible for the novel current-induced torque phase diagram that we discuss below.

Current-Induced Torques for Co/NiMn— We employ a non-equilibrium Green’s function (NEGF) approach [17] for microscopic calculations of magneto-transport properties and current-induced torques. Quasiparticle Hamiltonians are constructed using density functional theory

within the local spin density approximation (extended to allow noncollinear spin configurations), norm-conserving pseudopotentials, and an s , p , d single-zeta atomic orbital basis set. The induced torque per-current can be calculated atom by atom[17]:

$$\frac{\vec{S}}{I} = \frac{\mu_B}{e} \frac{\int dk_{\parallel} \sum_{\alpha,\beta} (\vec{\Delta}_{\alpha,\beta} \times \vec{m}_{\beta,\alpha}^{tr})}{\int dk_{\parallel} T(\epsilon_F)}. \quad (1)$$

The right-hand-side of Eq. (1) expresses the misalignment between the non-equilibrium spin-density, $\vec{m}_{\alpha,\beta}^{tr}$, and the spin-dependent part of the exchange-correlation potential, $\vec{\Delta}_{\alpha,\beta}$. Here $T(\epsilon_F)$ is the transmission probability, k_{\parallel} labels transverse channels, α, β are orbital labels, and α is summed only over orbitals centered on the atom of interest. When the many-body Hamiltonian is spin rotationally invariant, the current-induced torque on each atom is equal to the net spin flux out of the atom.

We apply this approach to a system with a single interface between antiferromagnetic NiMn and ferromagnetic Co. The crystal structure of NiMn is face centered tetragonal, with Ni and Mn layers alternating in the (001) direction[18]. The Ni atoms are approximately nonmagnetic, while the Mn atoms form a compensated antiferromagnetic 2-dimensional lattice within each plane (See Fig. (2)). In our calculation, we use $a = 3.697$ Å, with a c/a ratio of 0.9573 for NiMn and, following Ref. [19], a lattice-matched tetragonal structure for Co with a c/a ratio chosen to conserve its experimental atomic volume. The results shown here are for current in the (001) direction, perpendicular to the interface between Co and Ni terminated NiMn. The current through the interface has a polarization $P = (G_{\uparrow} - G_{\downarrow}) / (G_{\uparrow} + G_{\downarrow}) = 6.4\%$ when the F and AF moments are collinear, with the larger conductance for the ferromagnet majority spins. To evaluate the current-induced torques present in the system, we rotate the Co layer magnetization orientation by an angle θ with respect to the NiMn moment direction and use Eq. (1).

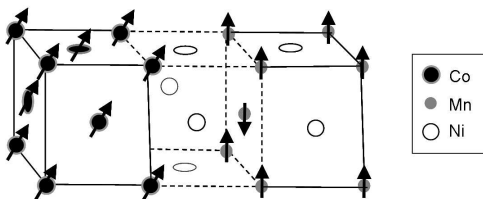


FIG. 2: Illustration of the NiMn-Co interface model.

Fig. (3) shows the total torques acting on the AF and F order parameters as a function of θ . The torque acting on the F closely follows the form anticipated on symmetry grounds above. We associate the small torque at $\theta = \pi/2$ with weak ferromagnetism which is induced in the top (Ni) layer of NiMn. In NiMn only the difference between the torques on the two sublattice of the AF

drives the order parameter. The current-induced torque tends to drive the orientation of downstream material (AF or F) parallel with that of the upstream, and to drive the upstream material orientation perpendicular to the downstream (so that for electron flow from AF to F, the F tends to align to AF, and the AF tends to become perpendicular to F, within their common plane).

We have also considered Mn terminated NiMn adjacent to Co. In this case the last Mn layer acquires a net magnetic moment in the direction of Co. The current-induced torques do not show as clean of a $\sin 2\theta$ behavior, but a combination of $\sin\theta$ and $\sin 2\theta$. We conclude that the absence of odd $n \sin n\theta$ torques is closely tied to the degree of compensation at the AF interface.

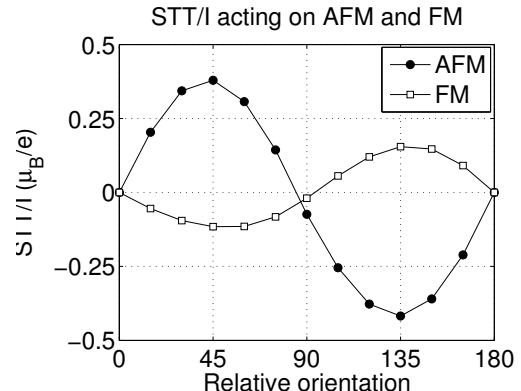


FIG. 3: Current-induced torques per current acting on the order parameters of the AF and F layers vs relative orientation. In the AF the order parameter is driven by the differences between torques on opposite sublattices. Units are μ_B/e .

Phase Diagram for a pinned antiferromagnet— We now consider the implications of this new form of current-induced torque for systems with the usual thin film geometry, assuming for the sake of definiteness that the AF moment direction \hat{n}_{AF} is pinned and lies in the plane, and that the external magnetic field H is applied in the same direction. We use a spherical coordinate system for the F moment direction, taking \hat{n}_{AF} as the polar direction and the \hat{x} direction as the film normal (the demagnetizing field is denoted by H_d). We assume that a non-magnetic spacer layer is placed between the F and AF layers which is sufficiently wide to make exchange interactions negligible. Just as in the pure F case, a spacer layer is not expected to have a large impact on current-induced torques. We also omit easy-axis anisotropy; its inclusion wouldn't substantially change the picture described below. With these ingredients the polar and azimuthal torques acting on the ferromagnet are:

$$\begin{aligned} \Gamma_{\theta} &= -\frac{1}{2} \sin(\theta) \sin(2\phi) H_d + \sin(2\theta) H_{CI} ; \\ \Gamma_{\phi} &= \sin(\theta) H + \frac{1}{2} \sin(2\theta) \cos^2(\phi) H_d . \end{aligned} \quad (2)$$

Here we have parameterized the current-induced torque by H_{CI} and chosen a sign convention in which $H_{CI} < 0$ when it favors perpendicular alignment. Steady-state solutions satisfy $\Gamma_\phi = \Gamma_\theta = 0$ and are stable for small deviations when Gilbert damping is included. We have determined the stability regions of the steady state solutions discussed below by following the procedure described in Ref. 20. We present all of our results in terms of the dimensionless fields $h = H/H_d$ and $h_{CI} = H_{CI}/H_d$.

For the geometry we consider, the behavior of \mathbf{F} is very simple in the absence of the current induced torques: the magnetization simply lines up with the magnetic field applied in the easy plane. The influence of the current-induced torque on \mathbf{F} is particularly dramatic for $H_{CI} < 0$. Because the torques then tend to push the magnetization perpendicular to \hat{n}_{AF} , the field-aligned solution is stable only for

$$h_{CI} \geq -\frac{\alpha}{2} \left(|h| + \frac{1}{2} \right), \quad (3)$$

where α is the Gilbert damping parameter. For sufficiently strong currents and external fields that are not too strong, a perpendicular-to-plane steady state becomes stable:

$$\begin{aligned} \theta &= \frac{\pi}{2} + h; \\ \phi &= -2h_{CI}h + n\pi. \end{aligned} \quad (4)$$

These equations have been derived assuming that h and h_{CI} are small. In the above n is an even integer for solutions which point approximately in the $+\hat{x}$ direction, and an odd integer for the $-\hat{x}$ direction. The region of stability for this solution is:

$$h_{CI} \leq -\frac{\alpha}{2} \left(\frac{h \sin h - 2 \cos^2 h}{h \sin h - \cos 2h} \right), \quad (5)$$

where the the fraction on the r.h.s. of the above inequality must be negative, implying that $|h| < 0.608$, or equivalently $|H| < \mu_0 M_s (0.608)$.

The stability of this counter-intuitive stable steady state is explained in Fig. (4). This figure illustrates the situation when the excursions from the easy plane are small. For simplicity we first consider no external field. In the absence of the current-induced torque a small fluctuation out of the easy plane would initiate precession about the hard axis which damps back into the easy plane. The presence of the $\sin 2\theta$ torque, however, drives the magnetization perpendicular to \hat{n}_{AF} within their common plane. As the magnetization orientation \hat{m} precesses around the hard-axis, this torque vector has a component which points out of the easy plane. If the angle between \hat{n}_{AF} and the in-plane component of \hat{m} is β , the magnitude varies as $\Gamma_x = 2H_{CI}m_x \sin^2 \beta$, as shown in the figure. The crucial point is that this torque is always positive throughout the precession. When this torque exceeds the damping, the out-of-plane configuration is stabilized. The eventual out-of-plane orientation

can be $+\hat{x}$ or $-\hat{x}$ depending on the direction of the initial fluctuation out of plane. The presence of an applied field changes the trajectory of the magnetization upon excursions from the easy-plane. For a sufficiently large applied field, the torque is unable to stabilize the out-of-plane configuration, and no steady state is reached.

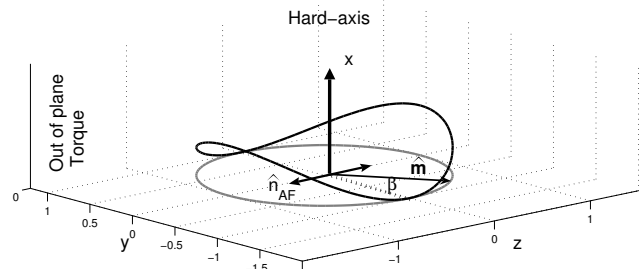


FIG. 4: Saddle shape illustrates the out-of-plane torque vs β for small excursions of the magnetization orientation \hat{m} from the easy plane. The out-of-plane torque is always positive.

Interesting new steady states can in principle also be induced by the current-induced torque for $H_{CI} > 0$. For $|H| \leq H_d$, the steady state stability analysis identified configurations in which the magnetization is approximately anti-aligned with the applied field:

$$\begin{aligned} \theta &= \cos^{-1}(-h) \\ \phi &= -2h_{CI}h. \end{aligned} \quad (6)$$

which is stable for the range of applied fields and currents

$$h_{CI} \geq \frac{\alpha}{2} \left(\frac{2 - h^2}{3h^2 - 1} \right) \quad (7)$$

For $H_{CI} > 0$ and $|H| \geq H_d$, the equilibrium solutions are $m_z = \pm 1$. In this case the solution and stability condition for steady state with magnetization anti-aligned with the field are:

$$\begin{aligned} m_z &= \frac{-H}{|H|}; \\ h_{CI} &\geq \frac{\alpha}{2} \left(|h| - \frac{1}{2} \right). \end{aligned} \quad (8)$$

This state only occurs if the magnetization is initially nearly anti-aligned with the applied field. The reason for its stability is that this form of the current-induced torque does not distinguish between $+\hat{z}$ and $-\hat{z}$ - it merely tends to make to direct the \mathbf{F} to the nearest available \hat{z} -axis, even if it's opposite to the applied field. The region for such a solution is shown in Fig. (5), labelled $\pm z$. It is seen that the applied field must be sufficiently large for this solution to be stabilized. This misaligned steady state may not be experimentally relevant however because it occurs only when the magnetization is initially nearly anti-aligned to an applied field of finite magnitude $|H| > H_d \sqrt{1/3}$.

Fig. (5) shows the x and z components of the magnetization as a function of applied field and current, determined numerically. We have taken the damping $\alpha = .01$, and the applied field and spin transfer torque are scaled by the demagnetization field H_d . Also shown is the magnitude of the power spectrum peak of $z(t)$ (labelled “P_Z”) - a nonzero value indicates a precessing solution. Also shown is the stability boundaries defined by Eqs. (3, 5, 7, 8). The numerics verify the stability of the unusual out-of-plane and field-anti-aligned solutions. The conversion of the dimensionless h_{CI} into a real current density for a material with demagnetization field of 1 T is $J = (h_{CI}t) \times 3.8 \cdot 10^9 \text{ A/cm}^2$, where t is the thickness of the F layer in nm.

The data for each (h, h_{CI}) point of Fig. (5) is obtained beginning from an initial condition close to the solution given by Eq. (4). These equilibrium solutions are not universal attractors, and are attained for a subset of initial conditions. To see the effect of initial conditions, we have also swept the applied field from negative to positive for each applied current, using the slightly perturbed final coordinates of a trajectory as the initial condition for the next value of applied field. The out-of-plane solution space is reduced, shown by the dotted line in Fig. (5) in the stability boundaries plot.

We now comment on the experimental possibilities of seeing these effects. In the preceding analysis, we assume that the AF is fixed. This can be accomplished by placing a large F adjacent to the AF, so that the AF is pinned via the exchange bias effect (the overall stack structure would be pinning F - AF - spacer - free F). The presence of this pinning F may influence the dynamics of the free F, but its signature should be very distinct from the influence of the AF layer on the free F. The orientation of the free F should be observable from magnetoresistance effects with the pinning ferromagnet.

A virtue of the out-of-plane F configuration is that the surface of the AF need not be single domain for its observation. As long as the magnetization of the AF is compensated and points in the plane (which is the preferred direction for NiMn [21, 22]), different orientations of domains at the AF surface should cooperatively push the F out of the plane. The encouraging aspect of this proposal is that the signature of the AF current-induced torque is so unique, helping to provide a distinguished characteristic for its observation.

FIG. 5: Magnetic configuration (M_x, M_z) and peak of power spectrum P_z (arbitrary units) versus applied field and current. Also shown is stability boundaries found analytically (the labels $\pm x, \pm z$ refer also to solutions which point approximately in these directions). The stability boundary plot also shows the reduced out-of-plane solution space for negative to positive field sweep with a dashed line.

Acknowledgments— We would like to acknowledge very helpful conversations with Maxim Tsoi and Olle Heinonen. This work was supported in part by Seagate Corporation and by the National Science Foundation under grant DMR-0606489, and the computational work was supported by Texas Advanced Computational Center (TACC).

-
- [1] Slonczewski, J. Magn. Magn. Mat. **62**, 123, (1996).
 - [2] L. Berger, Phys. Rev. B **54**, 9353 (1996).
 - [3] M. Tsoi *et al.*, Phys. Rev. Lett. **81**, 493(E) (1998).
 - [4] M. Tsoi *et al.*, Nature **406**, 46 (2000).
 - [5] J. A. Katine *et al.*, Phys. Rev. Lett. **84**, 3149 (2000).
 - [6] F. J. Albert *et al.*, Phys. Rev. Lett., **89**, 226802 (2002).
 - [7] M. R. Pufall *et al.*, App. Phys. Lett. **83**, 323 (2003).
 - [8] G. S. Beach *et al.*, Phys. Rev. Lett. **97**, 057203 (2006)
 - [9] J. Grollier *et al.*, Appl. Phys. Lett. **83**, 509 (2003).
 - [10] A. Yamaguchi *et al.*, Phys. Rev. Lett. **92**, 077205 (2004).
 - [11] M. Yamanouchi *et al.*, Nature **428**, 539 (2004).
 - [12] M. Hayashi *et al.*, Phys. Rev. Lett. **96**, 197207 (2006).
 - [13] A. S. Núñez *et al.*, Phys. Rev. B **73**, 214426 (2006).
 - [14] P. M. Haney *et al.*, Phys. Rev. B **75**, 174428 (2007).
 - [15] Z. Wei *et al.*, Phys. Rev. Lett. **98**, 116603 (2007).
 - [16] S. I. Kiselev *et al.*, Nature **425**, 380 (2003).
 - [17] P. M. Haney *et al.*, Phys. Rev. B **76**, 024404 (2007).
 - [18] L. Pál *et al.*, J. App. Phys. **39**, 538 (1968).
 - [19] T. C. Schulthess *et al.*, J. App. Phys. **83**, 7225 (1998).
 - [20] Ya. B. Bazaliy *et al.*, Phys. Rev. B **69**, 094421, (2004).

- [21] A. Sakuma, *J. Mag. Magn. Mat.* **187**, 105 (1998).
- [22] J.S. Kasper *et al.*, *J. Phys. Chem. Solids* **11**, 231 (1959).